Comparative Test ofTotal Suspended Solids(TSS) InSuwung Estuary Using Sentinel-2B and Landsat 8 Imagery

ABSTRACT

This study aims to determine and compare the accuracy of total suspended solids (TSS) estimates using Sentinel-2B and Landsat 8 satellite imagery in the Suwung estuary, Denpasar city, Bali. The TSS measurements in the laboratory were carried out on 20 samples for Sentinel-2B (Lab_S) and 20 samples for Landsat 8 (Lab_L) which were taken at the same coordinates. Regression and correlation methods are used to validate TSS estimates against laboratory TSS. Accuracy tests to determine the level of estimation error use root mean square error (RMSE), mean absolute error (MAE), and mean relative error (MRE). Comparison of estimation accuracy is determined by differences in error rate calculation results. The results of regression analysis and accuracy tests for paired samples show a very strong correlation, both in pair 1 (Lab_S with Sentinel-2B) namely r=0.9484 and in pair 2 (Lab_L with Landsat 8) it is r=0.8910, and the error rate for pair 1 is smaller than pair 2. The implications of these results show that the accuracy of the TSS estimation of the Laili algorithm using Sentinel-2B is better than Landsat 8.

Keywords: Comparative test, Total suspended solid (TSS), Suwung Estuaries, Sentinel-2B, Landsat-8.

1. INTRODUCTION

The Suwung Estuary is located in the southern part of Bali where it is the estuary of the Badung River which functions as a provider of clean water for the tourist destination area of South Bali which is very densely populated and therefore, attention to the condition and provision of clean water is crucial. More effective management in providing clean water, such as regular, sustainable and cost-effective monitoring, will be urgently needed in the future. Several physical parameters that can influence changes in water quality are turbidity (turbidity), electrical conductivity (EC), total dissolved solids (TDS), and total suspended solids (TSS) [1].

Total suspended solids (TSS) is an indicator for evaluating water quality. The majority of TSS in water bodies is caused by natural and human factors such as river runoff, coastal erosion, dredging, including rainfall, rising temperatures, wind, high waves, and all activities related to climate change [22]. The TSS value is directly proportional to turbidity which over a relatively long period of time can cause a buildup of sediment which ultimately results in shallowing of the water system and therefore, determining the TSS parameters in a water body is very important and a priority to ensure the quality of the water [29], [12], [17], [25].

The use of conventional methods in measuring water quality parameters periodically, is carried out by taking water samples in the field (in-situ), then testing them in the laboratory. The data produced is accurate, but it is often expensive, takes a relatively long time, requires a lot of energy, and is not comprehensive for studies on a large scale. An alternative method that is more effective, real time, comprehensive, cost-effective and sustainable that can be used is utilizing remote sensing satellite technology [8], [13], [18].

Remote sensing satellite technology products since the 1960s have been widely used by developed countries for monitoring the aquatic environment [18]. Many researchers use remote sensing satellite products such as SPOT, Sentinel-2, Landsat 8, Modis, Wordview 3 or Himawari-8 to monitor and evaluate water quality in various areas using TSS parameters [7], [6], [26], [14], [5], [27], [24], [15], [18], [4], [9], [13]. These studies validate the estimated value of satellite data generally using regression analysis, coefficient of determination (R^2), correlation coefficient (r) and testing the accuracy of estimates using statistical parameters such as root mean square error (RMSE), mean absolute error (MAE), normalized mean absolute error (NMSE) or mean relative error (MRE).

The RMSE value shows the size of the error from the difference between the estimated value and in-situ. The smaller the RMSE, the closer and more precise the estimated value is to in-situ data. MAE values with small estimation errors have high accuracy and NMAE shows the normalized error rate in percent (%), where NMAE values < 30% can be used as evidence of the validity of research image data [24]. The competency parameters R^2, r, and residual standard error (RSE) are used to assess and decide on one of several alternative models or algorithms used in estimating TSS in Indonesia based on Landsat 8 satellite data [29]. Integration of TSS estimates in the Suwung estuary using the Laili (2015) algorithm extracted from the Sentinel-2B acquisition of 16 June 2023 as variable x and in-situ data as variable y produces a regression model y=1.0213x – 0.2921, with R2 =0.993 [30].

The synergy of 2 satellite images, namely Landsat 8 OLI and Sentinel-2 MSI, which have different spatial resolutions, makes it possible to develop new algorithms for monitoring the dynamics of sensitive areas of water systems, and regression analysis on the TSS time series shows that the combination of the two sensors is very good, where the consistency of the green band reflectance provides the lowest difference in mean absolute percentage error (MAPE), namely 4.6% [10]. A comparative study of the chl-a algorithm modeling extracted from Landsat 8 and Sentinel-2B to estimate the distribution of chl-a in the waters of Kendari Bay produced an RMSE for Landsat 8 of 0.00010 and Sentinel-2B of 0.02656 [3]. Landsat 8 image accuracy outperforms Sentinel-2A by 31% in estimating TSS, and to improve accuracy, extensive algorithm development is needed, so that it can differentiate bio-optical water quality in reservoirs Chebara Dam [19], [2].

Apart from algorithm development, TSS estimation from satellite data generally depends on the accuracy of atmospheric corrections where the methods that are often used are dark object subtraction (DOS), flash atmospheric correction , and second simulation of a satellite signal in the solar spectrum-vector (radiative transfer 6SV) [26], [23]. The weak spectral reflectance response from the surface of water bodies results in the inversion reflectance received by the sensor being only the reflectance above the atmosphere or top of atmosphere (TOA). To eliminate the contribution of atmospheric effects or obtain bottom of atmosphere (BOA) reflectance, radiometric and atmospheric corrections are carried out where atmospheric corrections are carried out using the Dark Object Subtraction (DOS) method [6], [21], [26].

This study aims to compare the accuracy of TSS estimates based on the Laili algorithm extracted from Sentinel-2B and Landsat 8 satellite images. The accuracy comparison is based on the competence of the two satellite images in estimating TSS. Competency is determined by the results of regression analysis, namely R^2 and coefficient r, as well as the results of accuracy tests with the parameters RMSE, MAE and MRE. Higher R^2 and r values, as well as smaller accuracy parameter test results, indicate that the TSS estimation results

from the image data are closer to the laboratory data results, so they are better and suitable to be used to estimate TSS in the Suwung estuary.

2. METHODOLOGY

2.1. Data Collection and Processing

The research location is in the Suwung estuary, South Denpasar subdistrict, Denpasar city, Bali and astronomically, the research location is located at coordinates 115° 11' 16" – 115° 11' 22" East Longitude and 8° 43' 26"– 8° 44' 04" South Latitude. A map of the research location is presented in Figure 1a and an overview of the situation of the research sampling location is presented in Figure 1b. The time for taking water samples in the field is adjusted to the time of recording or acquisition of satellite image data, namely June 16 2023 for the Sentinel-2B sample and 24 June 2023 for the Landsat 8 sample. This was done so that the measurement results were real time. The number of samples for each tested was 20 which were taken at random observation points (OP) locations.

Figure 1a .Suwung estuary research location, Bali

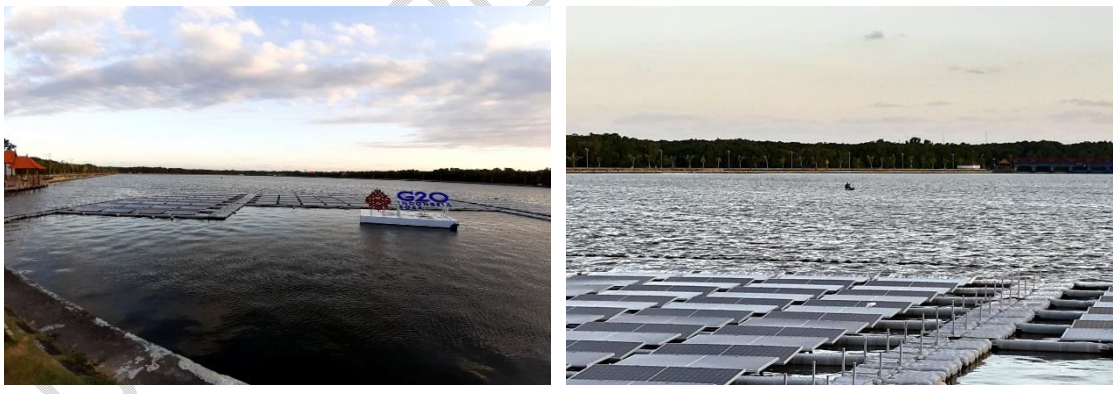

Figure 1b. Situation of the Suwung estuary research location , Bali

Field sample TSS measurements are measured in the laboratory using the gravimetric method which refers to the international standard water inspection method in accordance with PP No. 82, 2001 [20] using Equation (1).

$$TSS(mg/L) = \frac{(W_1 - W_0) \times 1000}{V_{sampel}} \quad (1)$$

Where:

W_0 = initial weight of filter paper (mg)
W_1 = final weight of filter paper after drying (mg)
V_{sample} = volume of sample (ml)

Image data collection from Sentinel-2B and Landsat 8 images has different acquisition times, but the TP of the samples tested is located in the same 50S zone universal transverse mercator (UTM) coordinates. The stages of processing satellite images to obtain estimated TSS values for each satellite image are:

1) Geometric correction and conversion of raw image pixels to top of atmosphere (TOA) reflectance values
2) Atmospheric correction using the DOS method which aims to obtain the BOA reflectance value, where the BOA reflectance value is also known as the remote sensing (Rrs) reflectance value [3].
3) Image cropping to obtain an image of the study area
4) Applying TSS algorithm using the formula as presented in Equation (2)[16].

$$TSS\left(\frac{mg}{L}\right) = 31.42\frac{(Log(R_{rs}\ Blue))}{(Log(R_{rs}\ Red))} - 12.719 \quad (2)$$

Where :

R_{rs}Blue is a reflectance remote sensing on the channel (band) blue
R_{rs}Red is a reflectance remote sensing on red band

Band of the Sentinel-2B image is in band 2 (central wavelength 0.490 μm), and in the Landsat 8 image it is also in band 2 (wavelength interval 0.45 – 0.51 μm). The red band of the Sentinel-2B image is in band 4 (central wavelength 0.665 μm), while in Landsat 8 it is also in band 4 (wavelength interval 0.64 – 0.67 μm).

2.2. Data analysis

The TSS validation test for the spectral model of Sentinel-2B and Landsat 8 satellite images in the laboratory used regression and correlation analysis, where as the independent variable (X) is TSS data from laboratory measurements and as the dependent variable (Y) is TSS estimation data from satellite images ([11], [26], [8]. The paired sample difference test was carried out using a two-way T test, and to test the accuracy or determine the error level of the two satellite image data in estimating TSS, in this study root mean square error (RMSE) analysis was used, mean absolute error (MAE) and mean relative error (MRE) where the formulas are presented as in Equations (3), (4) and (5) [22], [24].

$$RMSE = \sqrt{\frac{\sum_{i=1}^{n}(X_i - Y_i)^2}{n}} \quad (3)$$

$$MAE = \frac{1}{n}\sum_{i=1}^{n}|X_i - Y_i| \quad (4)$$

$$MRE = \frac{1}{n}\sum_{i=1}^{n}\left|\frac{X_i - Y_i}{X_i}\right| x\ 100\% \quad (5)$$

Where :

X=Laboratory TSS value
Y=TSS value of satellite imagery
n=Number of data and i=1..n

Comparison of estimates is determined by calculating the ratio of RMSE, MAE and MRE from the two types of satellite images in estimating TSS. The research flow diagram is presented in Figure 2.

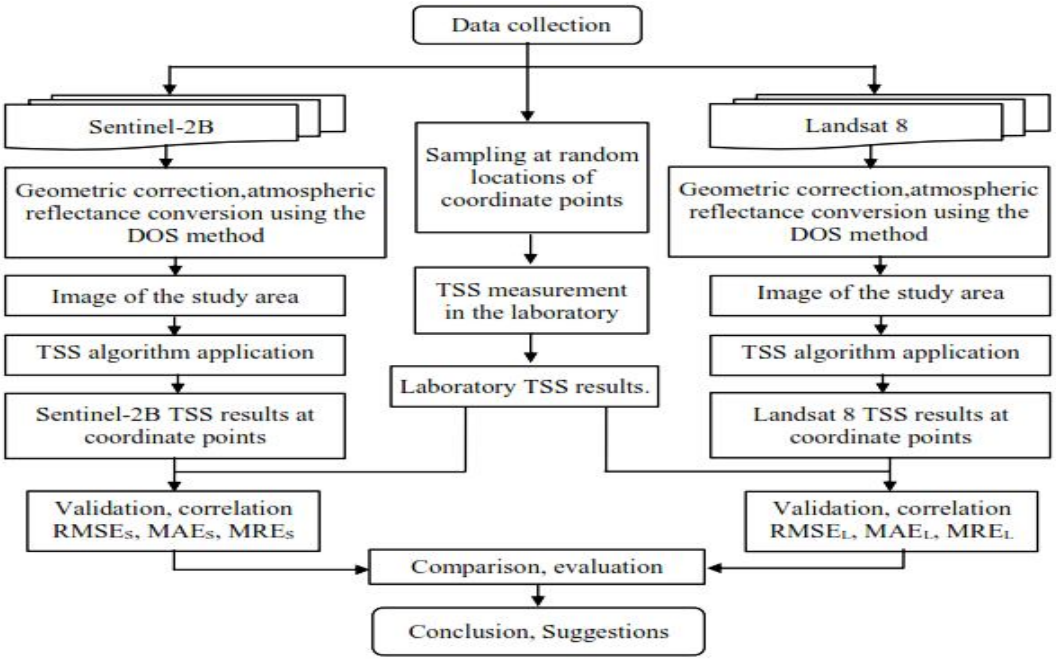

Figure 2. Research flow chart

3. RESULTS AND DISCUSSION

3.1. Results

The results of image processing and application of the TSS algorithm according to Equation (2) using the Terrset product image processing program, version 18.21 which are presented in the form of spatial information are shown in Figure 3a for Sentinel-2B imagery, while for Landsat 8 imagery in Figure 3b. Water quality parameter measurements represented by 20 TSS concentration samples in processed satellite image pixels for Sentinel-2B and the laboratory (Lab_S) as well as for Landsat 8 and the laboratory (Lab_L) are presented in Table 1. The validation graph for TSS estimates from image pixel measurements of laboratory TSS concentrations through linear regression analysis based on test data in Table 1 is presented in Figure 4a for Sentinel-2B image pixels and Figure 4b for Landsat 8.

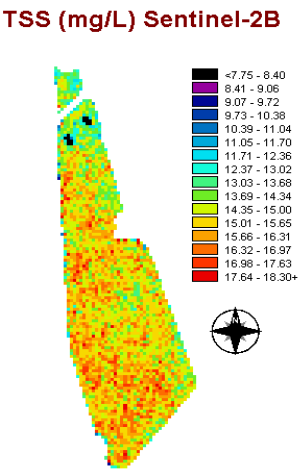

Figure 3a. Sentinel-2B TSS distribution

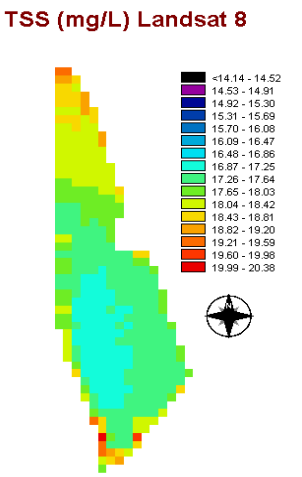

Figure 3b. Landsat 8 TSS distribution

Table 1. Results of TSS measurements from laboratories and satellite images

OP	Coordinates (m)		TSS Sentinel-2B (mg/L)		TSS Landsat 8 (mg/L)	
	Latitude	Longitude	Lab_S	Pixel value	Lab_L	Pixel value
1	300561.4	9034968.2	8.00	13.464	6.00	17.623
2	300564.7	9034876.5	7.00	12.258	5.00	17.597
3	300563.5	9034865.8	11.00	15.476	6.00	17.597
4	300748.6	9034943.6	8.00	13.726	9.00	17.930
5	300846.4	9034758.8	9.00	14.237	6.00	17.660
6	300875.9	9034655.7	8.00	13.819	5.00	17.558
7	300905.4	9034587.9	7.00	12.639	7.00	17.750
8	300917.3	9034557.2	10.00	14.416	9.00	18.152
9	300941.5	9034468.8	8.00	13.186	5.00	17.580
10	300973.4	9034378.3	9.00	14.903	6.00	17.653
11	300746.1	9034975.6	7.00	12.539	9.00	18.053
12	300695.4	9035145.7	8.00	13.121	10.00	18.218
13	300678.3	9035252.7	8.00	13.683	12.00	18.997
14	300562.9	9034938.7	13.00	15.704	6.00	17.623
15	300562.2	9034917.9	9.00	14.068	6.00	17.623
16	300579.9	9034732.9	7.00	12.068	9.00	17.916
17	300572.8	9034675.6	9.00	14.117	4.00	17.612
18	300581.8	9034554.8	14.00	16.121	12.00	18.062
19	300601.5	9034381.9	8.00	12.915	5.00	17.620
20	300670.6	9034153.3	15.00	17.277	14.00	19.538

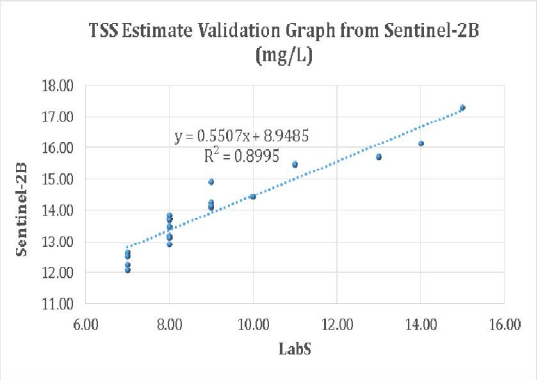

Figure 4a. Lab_STSS validation against Sentinel- 2B

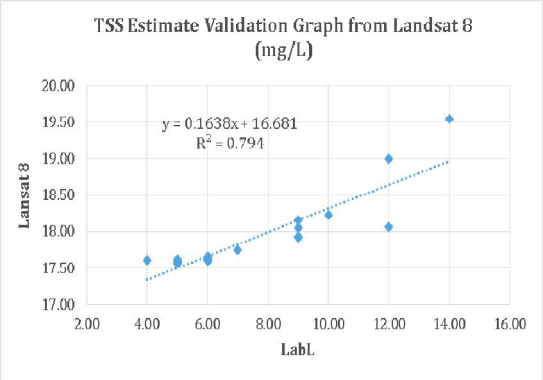

Figure 4b. Lab_L TSS validation against Landsat 8

A summary of the results of statistical analysis and correlation of paired samples, namely pair 1 (pair 1) which is a pair of TSS Lab_S with Sentinel-2B and pair 2 (pair 2), TSS Lab_L with Landsat 8 which was processed using IBM SPSS Statistics version 22 is presented in Table 2. Results of paired sample average tests and T test results are presented in Table 3.

Table 2. Paired Samples Statistics and Correlation

		Mean	N	Std. Deviation	Std. Error Mean	Correlation	Sig.
Pair 1	Lab_S	9.150	20	2.346	.525	.948	.000
	Sentinel-2B	13.987	20	1.362	.305		
Pair 2	Lab_L	7.550	20	2.799	.626	.891	.000
	Landsat 8	17.918	20	.515	.115		

Tabel 3. Paired Samples Test

	Paired Differences					t	df	Sig. (2-tailed)
	Mean	Std. Deviation	Std. Error Mean	95% Confidence Interval of the Difference Lower	Upper			
Pair 1	-4.837	1.139	.255	-5.370	-4.304	-18.989	19	.000
Pair 2	-10.368	2.353	.526	-11.469	-9,267	-19,706	19	,000

A comparison graph of the results of Lab_S TSS concentration measurements and estimates from Sentinel-2B at each observation point is shown in Figure 5a, while for Lab_L and Landsat 8 it is shown in Figure 5b.

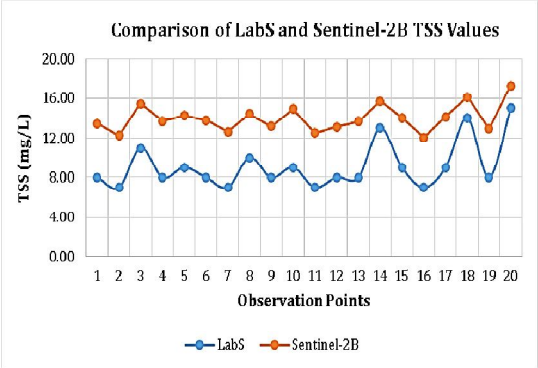

Figure 5a. Comparison of TSS Lab_S and Sentinel-2B

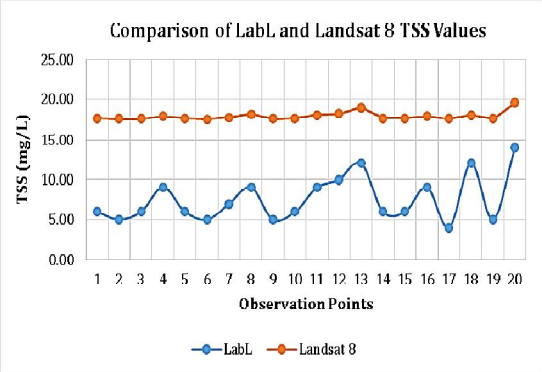

Figure 5b. Comparison of TSS Lab_L and Landsat 8

The results of the accuracy test calculations show that there are differences in estimation results with laboratory measurements using 3 statistical parameters RMSE, MAE and MRE such as Equations (3), (4) and (5) are shown in Table 4.

Table 4. Summary of results and comparison of RMSE, MAE and MRE TSS image estimation with laboratory

No.	Analyzed variables	RMSE	MAE	MRE (%)
1	Pair 1	4.963	4.837	0.577
2	Pair 2	10.619	10.368	1.648
	Comparison of pair 1 with pair 2	0.467	0.466	0.350

3.2. Discussion

The spatial information as presented in Figures 3a and 3b, represents the distribution of TSS estimates produced by Sentinel-2B and Landsat 8 images. Visually, it can be clearly observed that there is a difference in displaying the distribution of TSS estimates, where this difference is due to the two images having different resolutions. In this study, the pixel spatial resolution of the Sentinel-2B, band 2 and band 4 images is 10 m, while the spatial resolution of the Landsat 8, band 2 and band 4 images is 30 m. An area of 900 m^2 is only represented by 1 Landsat 8 pixel, (30 m x 30 m = 900 m^2), whereas in Sentinel-2B, it is represented by 9 pixels, (10 m x 9 m = 900 m^2). Therefore, it is said that the Sentinel-2B image has a higher spatial resolution than Landsat 8, so that when visualizing the image, the Sentinel-2B image will appear smoother or more detailed [3], [10].

The results of TSS estimation measurements at 20 OP from Sentinel-2B and Landsat 8 using the TSS algorithm Equation (2) provide different values from the results of laboratory TSS measurements, as presented in Table 1. Differences in the values of these measurement results can be caused, among other things, by atmospheric factors, where even though atmospheric corrections have been made to the satellite image data, which in this study used the DOS method, however, the influence of the atmosphere is still there [6], [21].

Validation of TSS estimation measurement results against laboratory measurement results analyzed using linear regression analysis to obtain graphs and validation equations (regression equations) as presented in Figure 4a for Sentinel-2B imagery and Figure 4b for Landsat 8 imagery. This validation equation can be used to estimate measurements TSS uses real time satellite imagery when laboratory measurements are not available. Figure 4a and Figure 4b also show the coefficient of determination value, namely for Sentinel-2B it is $R^2 = 0.8995$ and for Landsat 8 it is $R^2 = 0.7940$. The determinant coefficient value explains

the ability of laboratory measured TSS data (independent variable) to explain the estimated TSS value from satellite imagery (dependent variable) [8], [11]. Based on this, because the coefficient value of Sentinel-2B is greater than Landsat 8, namely 0.8995 > 0.7940, it can be said that, qualitatively, Sentinel2-B ability to explain TSS estimates is greater than that of Landsat 8. In estimating TSS, Sentinel-2B capability is 89.95% explained by laboratory measurement results while Landsat 8 is 79.40%.

From Table 2 it can be seen that the correlation coefficient value for Sentinel-2B is r=0.948 and for Landsat 8 it is r=0.891. The correlation coefficient value explains the strength of the relationship or correlation that occurs between the independent variable and the dependent variable [11]. It can be seen that, in both pairs, both pair 1 and pair 2, the results of TSS estimation data from satellite imagery are very strongly correlated with laboratory TSS data. The correlation between pair 1 is stronger than pair 2. Figure 5a shows the comparison curve of estimated TSS measurement results from Sentinel-2B imagery with laboratory measurement results at 20 observation points and Figure 5b shows the comparison curve for estimated TSS measurement results from Landsat 8 imagery with laboratory measurement results at 20 observation point. The differences in estimates of TSS measurement results using satellite imagery and laboratory measurement results, both for pair 1 and pair 2, can also be explained by the value of the T test results.

Two-tailed T test analysis with α=0.05 for paired samples are presented in Table 3. The estimated bias of measurement results, which is represented by the standard deviation value, for pair 1 is 1.139, which is smaller than for pair 2, which is 2.353. The calculatedt value for pair 1 is –18,989 and for pair 2 is –19.706. The absolute value of these two pairs is greater than the t table value= 2.093. This shows that there are differences in the estimated results of TSS measurements from satellite images and laboratory results in accordance with the data presented in Table 1.

The results of calculating the accuracy of TSS measurement estimates for Sentinel-2B and Landsat 8 images as presented in Table 4 show that pair 1 with values of RMSE=4.963, MAE= 4.837 and MRE=0.577 is smaller than the values for pair 2. This shows that the estimation error is smaller, resulting in a high level of accuracy in estimating TSS [24]. Based on the comparison of the results of these three statistical parameters, it can be interpreted that the estimated TSS measurement results using Sentinel-2B imagery are closer to the results of laboratory measurements. This also means that, in estimating TSS in the Suwung estuary, Bali, the accuracy of Sentinel-2B imagery is better and the error rate is smaller compared to Landsat 8 imagery.

Comparison of quantitative estimation accuracy between pair 1 and pair 2, namely for RMSE 4.963 versus 10.619 or 4.963/10.619=0.467 (46.7%), comparison for MAE=0.466 (46.6%) and for MRE=0.350%. From the results of the comparison values, based on the RMSE value it can be said that, 46.7% of the estimation results for pair 1 are better than pair 2, and based on the comparison of MAE values it can be said that 46.6% of the estimation results for pair 1 are better than pair 2, and based on the comparison The MRE value can be said to be only 0.350%, the estimated results of pair 1 are better than pair 2. Another implication of the accuracy calculation results is that, the form of the regression equation model produced by Sentinel-2B on laboratory results in measuring TSS, namely Y = 1.6335X – 13.697 is more feasible and better to use in estimating TSS in the Suwung estuary compared to that produced by Landsat 8.

4. CONCLUSION

Based on the results and analysis where the RMSE, MAE and MRE values in pair 1 ($Lab_S$and Sentinel-2B imagery) are smaller than pair 2 (Lab_L and Landsat 8 imagery) it can be concluded that the accuracy of the TSS estimation of the Laili algorithm in the Suwung estuary using Sentinel-2B imagery is better than Landsat 8

imagery. Suggestions for developing this research are besides using satellite imagery which has a higher spatial resolution than Sentinel-2B, also applying other and appropriate TSS algorithms or developing existing algorithms so that they can provide more accurate TSS estimation results.

REFERENCES

[1] Abdullah, H.S., Mahdi, M.S., & Ibrahim, H.M. (2016). Water Quality Assessment Models for Dokan Lake Using Landsat 8 OLI Satellite Images. *Journal of Zankoy Sulaimani-Part A*, *19*(3), 25-42.https://doi.org/10.17656/jzs.10630

[2] Adawiah, S.W., Setiawan, K., Parwati, E., &Faristyawan, R. (2021). Development of Empirical Model of Total Suspended Solid (TSS) by using Landsat 8 on the Coast of Bekasi Regency. *IOP Conf. Series: Earth and Environmental Science 750 (2021) 012039*. https://doi.org/10.1088/1755-1315/750/1/012039

[3] Azharuddin, M., Usman, I., &Nurgiantoro. (2020). Comparative Study of Chl-a Algorithm Modeling Using L8 and S2b Image Data. JAGAT (Journal of Geography Applications and Technology), 4(1), 25-38. https://doi.org/10.5281/zenodo.3871265

[4] Baktiar, A. H., & Basith, A. (2020). Analysis of Total Suspended Solid (TSS) Content Using Worldview 3 Satellite Imagery in Karimunjawa Waters. Ellipsoid: Journal of Geodesy and Geomatics. 3(2), 112–118. https://doi.org/10.14710/elipsoid.2020.9210

[5] Bioresita, F., Pribadi, C.B., Firdaus, H.S., Hariyanto, T., & Puissant, A. (2018). The Use of Sentinel-2 Imagery for Total Suspended Solids (TSS) Estimation in Porong River, Sidoarjo. Ellipsoids: Journal of Geodesy and Geomatics, 1(1), 1–6. https://doi.org/10.14710/elipsoid.2018.2726

[6] Bui, Q.-T., Jamet, C., Vantrepotte, V., Meriaux, X., Cauvin, A., &Mograne, M. A., (2022). Evaluation of Sentinel-2/MSI Atmospheric Correction Algorithms over Two Contrasted French Coastal Waters. Remote Sens., 14, 1099. https://doi.org/10.3390/rs14051099

[6] Dhannahisvara, A.J., Harjo, H., Wicaksono, P., & Nugroho, F.S. (2018). Total Suspended Solid Distribution Analysis Using SPOT-6 Data InSegara Anakan, Cilacap. Geoplanning: Journal of Geomatics and Planning, 5(2), 177-188.

https://doi.org/10.14710/geoplanning.5.2.177-188

[7] Fathiyah, N., Pin, T.G., & Saraswati, R. (2017). Spatial and Temporal Patterns of Total Suspended Solid (TSS) with SPOT Imagery in the Cimandiri Estuary, West Java. 8th Industrial Research Workshop and National Seminar - ID, Bandung, Indonesia. https://doi.org/10.35313/IRWNS.V8I3.600

[8] Fernanda M. C. Pizani, F.M.C., Maillard, P., Ferreira, A.F.F., & de Amorim, C.C. (2020). ESTIMATION OF WATER QUALITY IN A RESERVOIR FROM SENTINEL-2 MSI AND LANDSAT-8 OLI SENSORS. ISPRS Annals of the Photogrammetry, Remote Sensing and Spatial Information Sciences, V(3), XXIV ISPRS Congress, 2020 edition. https://doi.org/10.5194/isprs-annals-V-3-2020-401-2020

[9] Hafeez, S., Wong, M. S., Abbas, S., & Jiang, G. (2021). Assessing the Potential of Geostationary Himawari-8 for Mapping Surface Total Suspended Solids and Its Diurnal Changes. Remote Sens. 13, 336. https://doi.org/10.3390/rs13030336

[10] Hafeez, S., Wong, M. S., Abbas, S., & Asim, M. (2022). Evaluating Landsat-8 and Sentinel-2 Data Consistency for High Spatiotemporal Inland and Coastal Water Quality Monitoring. Remote Sens., 14, 3155. https://doi.org/10.3390/rs14133155

[11] Hariyanto, T., Krisna, T. C., Khomsin, Pribadi, C. B., & Anwar, N. (2017). Development of Total Suspended Sediment Model using Landsat-8 OLI and In-situ Data at the Surabaya Coast, East Java, Indonesia. Indonesian Journal of Geography, 49(1), 73-79. http://dx.doi.org/10.22146/ijg.12010

[12] Hendrawan, I. G., Uniluha, D., &Maharta, I.P.R.F. (2016). Characteristics of Total Suspended Solids and Turbidity Vertically in the Waters of Benoa Bay, Bali. Journal of Marine and Aquatic Sciences, 2(1), 29-33. https://doi.org/10.24843/jmas.2016.v2.i01.29-33

[13] Imran, U., Zaidi, A., Mahar, R. B., & Khokhar, W.A. (2022). Assessment of the lake water quality using Landsat 8 OLI imagery: a case study of Manchar Lake, Pakistan. Arabian Journal of Geosciences, 1(15), 1094. https://doi.org/10.1007/s12517-022-10372-3

[14] Indeswari, L., Hariyanto, T., &Pribadi, C.B. (2018). Mapping the Distribution of Total Suspended Solids (TSS) Using Multitemporal Landsat Imagery and In Situ Data (Case Study: Porong River Estuary Waters, Sidoarjo). ITS Engineering Journal, 7(1), 2337-3520. https://doi.org/10.12962/J23373539.V7I1.28698

[15] Kurniadin, N., & Maria, E. (2020). Evaluation of the Total Suspended Solid (TSS) Algorithm on Landsat 8 Imagery Against In-Situ TSS Data. Ellipsoid: Journal of Geodesy and Geomatics. 3(1), 64–70. https://doi.org/10.14710/elipsoid.2020.6754

[16] Laili, N., Arafah, F., Jaelani, L.M., Subehi, L., Pamungkas, A., Koenhardono, E.S., &Sulisetyono, A. (2015). DEVELOPMENT OF WATER QUALITY PARAMETER RETRIEVAL ALGORITHMS FOR ESTIMATING TOTAL SUSPENDED SOLIDS AND CHLOROPHYLL-A CONCENTRATION USING LANDSAT-8 IMAGERY AT POTERAN ISLAND WATER. ISPRS Annals of the Photogrammetry, Remote Sensing and Spatial Information Sciences, II-2/W2. https://doi.org/10.5194/isprsannals-II-2-W2-55-2015

[17] Maulana, L., Suprayogi, A., & Wijaya, A.P. (2015). Analysis of the Effect of Total Suspended Solids in Determining the Depth of Shallow Seas Using the Van Hengel and Spitzer Algorithm Method. Undip Geodesy Journal, 4(2), 139-148. https://doi.org/10.14710/jgundip.2015.8512

[18] Neves, V. H., Pace, G., Delegido, J., & Antunes, S. C. (2021). Chlorophyll and Suspended Solids Estimation in Portuguese Reservoirs (Aguieira and Alqueva) from Sentinel-2 Imagery. Water, 1(13), 2479. https://doi.org/10.3390/w13182479

[19] Ouma, Y.O., Kimutai Noor, K., & Herbert. K. (2020). Modeling Reservoir Chlorophyll-a, TSS, and Turbidity Using Sentinel-2A MSI and Landsat-8 OLI Satellite Sensors with Empirical Multivariate Regression. Journal ofSensors, 2020(1), 1-21. https://doi.org/10.1155/2020/8858408

[20] PeraturanPemerintahRepublik Indonesia Nomor 82Tahun 2001 tentangPengelolaanKualitas Air Dan PengendalianPencemaran Air. https://www.regulasip.id/book/861/read

[21] Rees, W. G. (2012). Physical Principles Of Remote Sensing. 2nd Edition. UK: Cambridge University Press. https://doi.org/10.1017/CBO9780511812903

[22] Sa'ad, F.N.A.; Tahir, M.S., Jemily, N.H.B., Ahmad, A., &Amin, A.R.M. (2021). Monitoring Total Suspended Sediment Concentration in Spatiotemporal Domain over TelukLipat Utilizing Landsat 8 (OLI). Appl. Sci., 11, 7082. https://doi.org/10.3390/app11157082

[23] Soria-Perpinya, X., Delegido, J., Urrego, E.P., Ruiz-Verdu, A., Soria, J.M., Vicente, E., &Moreno, J. (2022). Assessment of Sentinel-2-MSI Atmospheric Correction Processors and In Situ Spectrometry Waters Quality Algorithms. Remote Sens., 14, 4794. https://doi.org/10.3390/rs14194794

[24] Siregar, E. S. Y., Rahimah, I., Siregar, V.P., Agus, S. B. (2019). Accuracy Test of Total Suspended Solid Concentration by Landsat 8 on In-Situ Data in Lancang Island

Waters, KepulauanSeribu. Proc. SPIE 11372, Sixth International Symposium on LAPAN-IPB Satellite. Bogor, Indonesia. https://doi.org/10.1117/12.2542758

[25] Sukmono, A. (2018). Pemantauan Total Suspended Solid (TSS) Waduk Gajah MungkurPeriode 2013-2017 Dengan Citra Satelit Landsat-8. Elipsoida : Jurnal Geodesi dan Geomatika, 1(1), 33–38. https://doi.org/10.14710/elipsoida.2018.2812

[26] Wang, C., Chen, S., Li, D., Wang, D., Liu, W., & Yang, J. (2017). A Landsat-based model for retrieving total suspended solids concentration of estuaries and coasts in China. Geosci. Model Dev., 10, 4347–4365, https://doi.org/10.5194/gmd-10-4347-2017

[27] Wibisana, H., Wardhani, P.C., &Masliyah. (2022). Analysis of The Distribution of Total Suspended Solids on The Coastal Sampang Coast Due To The Blega River Flow Using Satellite Image Data. 3rd International Conference Eco-Innovation in Science, Engineering, and Technology, Vol. 2022. http://dx.doi.org/10.11594/nstp.2022.2701

[29] Wijaya, D.R.P., Haribowo, R., & Ball, J.E. (2023). An Alternative Model to Estimate Total Suspended Solids Concentrations using Landsat 8 Imagery in Indonesia. Civil and Environmental Science Journal, 6(2). https://doi.org/10.21776/civense.v6i2.404

[30] Yuliara, I. M., Ratini, N.N., &Kasmawan, I.G.A. (2023). Integration of Sentinel-2A Imagery and Laboratory Measurements for Estuarine Pb and TSS Concentration Monitoring in Suwung, Denpasar City, Indonesia. Asian Journal of Research and Reviews in Physics, 7(4),68-73. https://doi.org/10.9734/AJR2P/2023/v7i4150